World Journal of Gastroenterology

Online Submissions: http://www.wjgnet.com/esps/
bpgoffice@wjgnet.com
doi:10.3748/wjg.v20.i17.5066

World J Gastroenterol 2014 May 7; 20(17): 5066-5073
ISSN 1007-9327 (print) ISSN 2219-2840 (online)

BRIEF ARTICLE

Solitary fibrous tumors in abdomen and pelvis: Imaging characteristics and radiologic-pathologic correlation

Xue-Ming Li, Jing Reng, Peng Zhou, Ying Cao, Zhu-Zhong Cheng, Yan Xiao, Guo-Hui Xu

Xue-Ming Li, Jing Reng, Peng Zhou, Ying Cao, Zhu-Zhong Cheng, Yan Xiao, Guo-Hui Xu, Department of Radiology, Sichuan Cancer Hospital, Chengdu 610041, Sichuan Province, China
Author contributions: Li XM and Xu GH designed the study and wrote the manuscript; Cheng ZZ and Xiao Y coordinated and provided the collection of all human and clinical materials; Reng J, Zhou P and Cao Y revised the manuscript.
Correspondence to: Dr. Guo-Hui Xu, MD, Department of Radiology, Sichuan Cancer Hospital, No. 55, Lane 4, RenMin Road (South), Chengdu 610041, Sichuan Province, China. xgh0913@hotmail.com
Telephone: +86-28-85420198 Fax: +86-28-85420195
Received: October 22, 2013 Revised: January 8, 2014
Accepted: March 5, 2014
Published online: May 7, 2014

Abstract

AIM: To describe the imaging features of solitary fibrous tumors (SFTs) in the abdomen and pelvis, and the clinical and pathologic correlations.

METHODS: Fifteen patients with pathologically confirmed SFTs in the abdomen and pelvis were retrospectively studied with imaging techniques by two radiologists in consensus. Patients underwent unenhanced and contrast-enhanced imaging, as follows: 3 with computed tomography (CT) and magnetic resonance imaging (MRI) examination, 8 with CT examination only, and 4 with MRI examination only. Image characteristics such as size, shape, margin, attenuation or intensity, and pattern of enhancement were analyzed and correlated with the microscopic findings identified from surgical specimens. In addition, patient demographics, presentation, and outcomes were recorded.

RESULTS: Of the 15 patients evaluated, local symptoms related to the mass were found in 11 cases at admission. The size of the mass ranged from 3.4 to 25.1 cm (mean, 11.5 cm). Nine cases were round or oval, 6 were lobulated, and 10 displaced adjacent organs. Unenhanced CT revealed a heterogeneous isodense mass in 7 cases, homogeneous isodense mass in 3 cases, and punctuated calcification in one case. On MRI, most of the lesions (6/7) were heterogeneous isointense and heterogeneous hyperintense on T1-weighted images and T2-weighted images, respectively. All tumors showed moderate to marked enhancement. Heterogeneous enhancement was revealed in 11 lesions, and 7 of these had cysts, necrosis, or hemorrhage. Early non-uniform enhancement with a radial area that proved to be a fibrous component was observed in 4 lesions, which showed progressive enhancement in the venous and delayed phase. No statistical difference in the imaging findings was observed between the histologically benign and malignant lesions. Three patients had local recurrence or metastasis at follow-up.

CONCLUSION: Abdominal and pelvic SFTs commonly appeared as large, solid, well-defined, hypervascular masses with variable degrees of necrosis or cystic change that often displaced adjacent structures.

Key words: Abdominal imaging; Solitary fibrous tumors; Computed tomography; Magnetic resonance imaging

Core tip: Few studies have investigated the imaging features of solitary fibrous tumors (SFTs) in the abdomen and pelvis. We present the computed tomography and/or magnetic resonance imaging features of fifteen cases, and correlated them with histopathological results. We found that the imaging features of abdominal and pelvic SFTs predominantly appeared as large, well-defined, hypervascular masses with variable degrees of necrosis, cystic change, or hemorrhage that tended to displace adjacent structures. SFTs usually manifested as heterogeneous hyperintensity on T2-weighted images with low signal intensity areas representing flow voids, fibrosis, or collagen.

SFTs should be considered when the aforementioned imaging features are encountered.

Li XM, Reng J, Zhou P, Cao Y, Cheng ZZ, Xiao Y, Xu GH. Solitary fibrous tumors in abdomen and pelvis: Imaging characteristics and radiologic-pathologic correlation. *World J Gastroenterol* 2014; 20(17): 5066-5073 Available from: URL: http://www.wjgnet.com/1007-9327/full/v20/i17/5066.htm DOI: http://dx.doi.org/10.3748/wjg.v20.i17.5066

INTRODUCTION

Solitary fibrous tumors (SFTs) were first described by Klemperer and Rabin in 1931 as a localized fibrous mesothelioma[1]. The origin of SFTs has been controversial, and it is now considered to be a pathologically diverse, ubiquitous mesenchymal neoplasm of fibroblastic or myofibroblastic origin that can be either benign or malignant[2,3]. Clinically, they are often misdiagnosed as other hypervascular tumors by radiological and pathologic examination. Although SFTs may occur in any site of the body, they have been predominantly localized in the pleura, followed by the head and neck, and their presence in the abdomen and pelvis is rare.

Although the histopathological features of SFTs are well characterized, the appearance of these tumors on imaging is not well documented. To date, the most extensive reports regarding the imaging characteristics of SFTs in the abdomen and pelvis is by Shanbhogue *et al*[4], Zhang *et al*[5], and Ginat *et al*[6], and others focused on case reports[7-10]. To better characterize the radiological features of this rare disease, we present the computed tomography (CT) and/or magnetic resonance imaging (MRI) features of 15 cases of SFTs within the abdomen and pelvis, and correlated them with the histopathological findings. To our knowledge, this is the largest and most detailed radiologic case series reported to date for SFTs.

MATERIALS AND METHODS

Study population and imaging protocol

CT and MRI findings of 15 patients with pathologically confirmed SFTs in the abdomen and pelvis were retrospectively reviewed. Of these 15 patients, three underwent both CT and MRI examination, 8 had CT examination only, and 4 had MRI examination only. This study was conducted according to the ethical standards of our institution and was approved by our review board.

Due to the retrospective nature of the study, the CT and MR images were acquired with varied parameters. Contrast-enhanced CT was acquired 45-60 s after intravenous injection of Ominipaque-based CT contrast agent; and contrast enhanced MRI scans were acquired 25-30 s (arterial phase), 45-60 s (venous phase), and 3 min (delayed phase) after intravenous administration of gadolinium-based MRI contrast agent. For CT examinations, patients were scanned using a 64 multi-detector CT (Lightspeed VCT, GE Healthcare, Chalfont St Giles, United Kingdom) with an X-ray tube voltage of 120 kV, current of 200 mA, width of collimator 64 mm × 0.625 mm, and collimation and intervals of 5-10 mm. MRI scans were performed with a 1.5 T scanner (Avanto, Siemens Medical Systems, Munich, Germany). The scanning parameters were as follows: a T1-weighted gradient-echo sequence (TR: 90-180 ms, TE: 2-5 ms, flip angle: 70°), T2-HASTE sequence (TR: 4000-6000 ms, TE: 80-100 ms, flip angle: 20°), and T1-weighted VIBE sequence (TR/TE: 4.8/2.2 ms, flip angle: 70°).

Imaging analysis

The images were reviewed by two radiologists working in consensus-one with 20 years of experience in abdominal imaging and one a fellow. Each was only aware of the histological diagnosis, but did not review the official preoperative radiology reports. The CT and MR images were evaluated for location, size, shape, margin, internal architecture, CT density, and MRI signal intensity compared with adjacent muscle, pattern of enhancement, and changes in adjacent structures. The degree of mass enhancement was assessed subjectively and categorized as follows: mild, when the enhancement was similar to that of adjacent muscle; moderate, when the enhancement was higher than that of muscle but lower than that of blood vessels; marked, when the enhancement was approaching that of blood vessels. These imaging findings were correlated with the microscopic findings of the surgically obtained specimens, and compared between the histologically benign and malignant groups. In addition, review of the patients' charts was performed to determine demographic data, clinical presentation, and postsurgical outcome.

RESULTS

Clinical results

The study group consisted of 12 men and 3 women with a median age of 65.2 years (range, 1-76 years). Of these 15 patients, 11 (73%) had local symptoms at admission, including a palpable mass (n = 4), abdominal pain or discomfort to various degrees (n = 5), difficulty in defecation (n = 3), urinary frequency or retention (n = 4), gross hematuria (n = 1), and a sexual disorder (n = 1). A firm and non-tender mass was revealed in 10 patients upon digital rectal examination. However, none had systemic symptoms; and all the routine laboratory studies were unremarkable. A Foley catheter was placed in the urethra with complete resolution of urinary symptoms in patients with urinary retention. Surgical excision was successfully performed in all patients; and embolization prior to surgery was performed in one patient to prevent excessive surgical hemorrhage. At follow-up 0-62 mo (median, 20.3 mo) after surgery, 2 patients had local recurrence and one had hepatic metastasis, and all were classified as malignant at initial pathological examination.

Table 1 Radiological findings of the 15 cases with solitary fibrous tumors

No/age/sex	Benign/ malignant	Location	Size (cm^2)	Shape, margin	CT density/MRI intensity	Degree, pattern of enhancement
1/1/M	Benign	Adrenal region-L	3.4 × 3.4	Rounded, well-defined	Isodensity with dot calcification	Moderate, homogeneous
2/76/M	Benign	Pararectal space-L	4.0 × 4.1	Oval, well-defined	Homogeneous isodensity	Moderate, homogeneous
3/39/M	Benign	Rectovesical space	11.3 × 11.5	Lobulated, well-defined	Isodensity with patchy necrosis	Marked, heterogeneous
4/41/M	Benign	Paravesical space-R	10.8 × 14.0	Oval, well-defined	Isodensity with patchy necrosis	Moderate, heterogeneous
5/29/F	Benign	Paravesical space-L	8.1 × 6.3	Oval, well-defined	Homogeneous isodensity Homogeneous isointensity (T1WI) Homogeneous hyperintensity (T2WI)	Marked, homogeneous
6/43/F	Benign	Presacral space	15.3 × 18.0	Oval, well-defined	Isodensity with patchy necrosis Heterogeneous isointensity with patchy hyperintensity (T1WI) Heterogeneous hyperintensity with patchy hypointensity (T2WI)	Marked, heterogeneous
7/60/F	Benign	Intraperitoneal	18.0 × 20.2	Lobulated, well-defined	Heterogeneous isointensity with patchy hypointensity (T1WI) Heterogeneous hyperintensity (T2WI)	Marked, heterogeneous Progressive enhancement
8/33/M	Benign	Presacral space	11.3 × 12.0	lobulated, well-defined	Isointensity with radial hypointensity (T1WI) Heterogeneous hyperintensity with radial hypointensity (T2WI)	Marked, heterogeneous Progressive enhancement
9/69/M	Malignant	Retroperitoneal	15.3 × 20.8	Lobulated, ill-defined	Isodensity with patchy necrosis	Moderate, heterogeneous
10/59/M	Malignant	Prevesical space	9.3 × 10.2	Oval, well-defined	Homogeneous isodensity	Moderate, homogeneous
11/52/M	Malignant	Intraperitoneal	7.4 × 8.1	Lobulated, well-defined	Isodensity with patchy necrosis	Marked, heterogeneous
12/61/M	Malignant	Paravesical space-R	11.6 × 12.0	Oval, well-defined	Isodensity with patchy necrosis	Marked, heterogeneous
13/47/M	Malignant	Rectovesical space	10.4 × 11.3	Oval, well-defined	Isodensity with patchy necrosis Heterogeneous isointensity with patchy hypointensity (T1WI) Heterogeneous hyperintensity (T2WI)	Moderate, heterogeneous
14/51/M	Malignant	Retroperitoneal	15.0 × 25.1	Lobulated, ill-defined	Heterogeneous isointensity with patchy hypointensity (T1WI) Heterogeneous hyperintensity (T2WI)	Marked, heterogeneous Progressive enhancement
15/57/M	Malignant	Rectovesical space	4.7 × 4.8	Oval, well-defined	Isointensity with radial hypointensity (T1WI) Heterogeneous hyperintensity with radial hypointensity (T2WI)	Marked, heterogeneous Progressive enhancement

M: Male; F: Female; L: Left; R: Right; CT: Computed tomography; MRI: Magnetic resonance imaging; T1WI: T1-weighted imaging; T2WI: T2-weighted imaging.

Imaging findings

The CT and MR imaging features of the 15 patients with SFTs are shown in Table 1. Three masses were found in the upper abdominal retroperitoneum, 2 in the peritoneal cavity, and 10 in the pelvis including 2 in the presacral space, one in the pararectal space, 3 in the rectovesical space, 3 in the paravesical space, and one in the prevesical space. All patients demonstrated a solitary mass with sizes ranging from 3.4 cm × 3.4 cm to 25.1 cm × 15.0 cm, with 10 masses larger than 10 cm in maximum diameter. Thirteen cases were well-defined, and 2 were ill-defined; 9 cases were round or oval, and the other 6 were lobulated. Thirteen cases displaced and compressed the adjacent organs, such as the pancreas, prostate, uterus, bladder, intestine, or vessels, and could not be delineated on CT and MR imaging. In addition, one of the patients with ill-defined margins showed invasion of the posterior stomach wall and envelopment of the celiac trunk and its branches (Figure 1). However, no lymphadenopathy or distant metastases were detected on the CT and MR images at initial evaluation.

On unenhanced CT images, all 11 cases with CT scans manifested as an isodense mass, of which 7 had relatively hypodense necrotic or cystic areas, 3 were homogeneous, and one had punctuated calcification. In total, 7 patients underwent MRI scans. On T1-weighted images, almost all lesions were isointense, in which 5 cases exhibited mostly isointense signals with patchy or radial areas of low intensity (Figure 2A), one case had mostly an isointense signal with a patchy area of mild hyperintensity (Figure 3A), and one case had homogeneous isointensity. On T2-weighted images (T2WI), one lesion exhibited homogeneous hyperintensity, and the others had heterogeneous hyperintensity, in which 3 cases had a patchy or radial area of hypointensity (Figures 2B, 3B). In addition, intra- or extra-tumoral flow voids were found in 4 cases on T2WI (Figure 2B).

After intravenous injection of contrast material, feeding vessels (vascular pedicle) were seen in 4 of the 15 cases (26.7%) (Figure 2C). The degree of mass enhancement on CT and MRI varied from moderate to marked; and in patients with MRI examination, it was marked in the arterial phase and persisted in the portal venous and delayed phase. Of these 15 cases, homogenous enhancement was

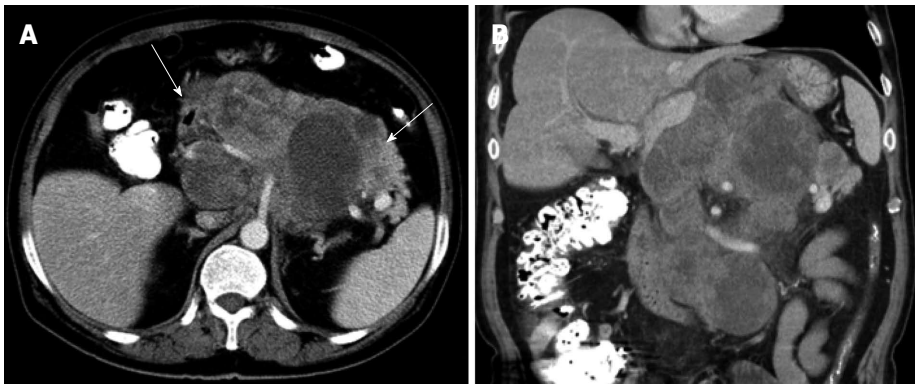

Figure 1 Computed tomography findings of a solitary fibrous tumor in the retroperitoneum. A: Contrast-enhanced axial image showing a lobulated, ill-defined, and heterogeneously moderate enhancing mass in the retroperitoneum. The mass invades the pancreas and stomach (arrows), and the celiac trunk and its branches were enveloped; B: The contrast-enhanced coronal reconstruction image shows envelopment of the branches of the celiac trunk.

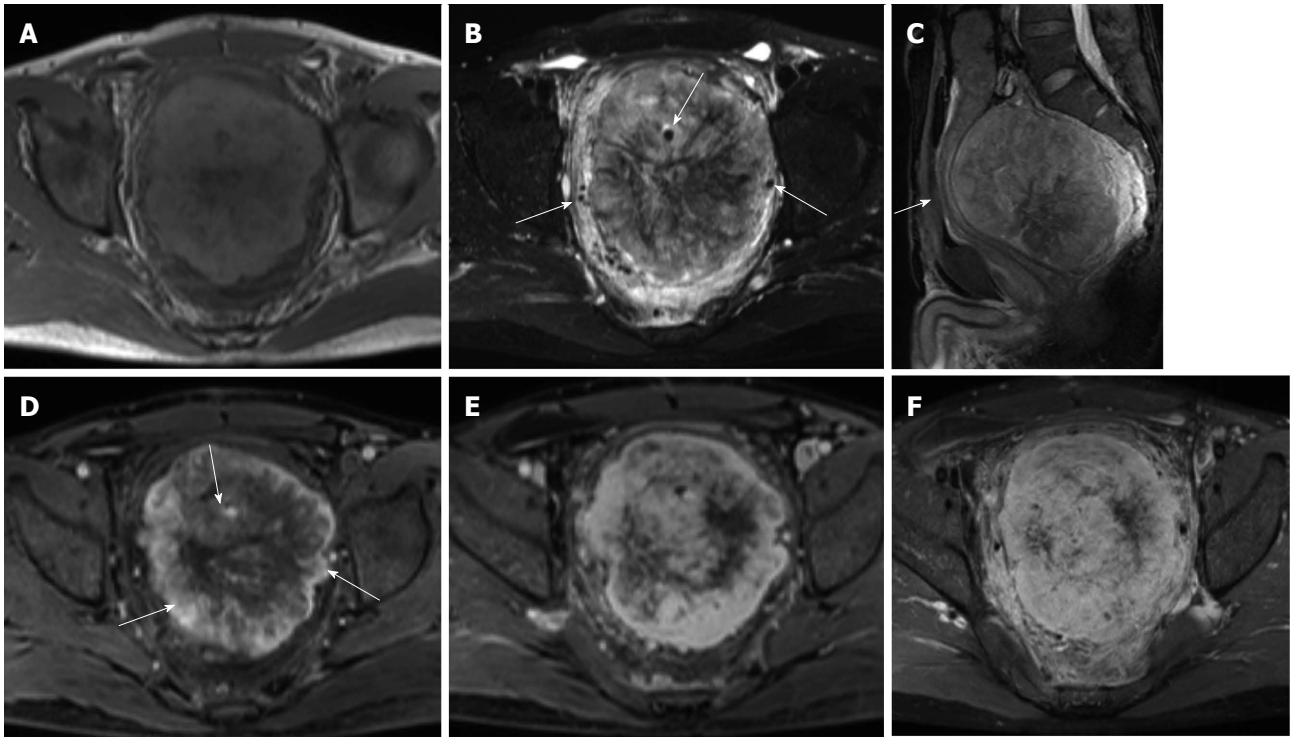

Figure 2 Magnetic resonance images of a solitary fibrous tumor in the presacral space. A: T1-weighted Magnetic resonance (MR) image showed that the mass is lobulated and almost isointense to the muscle. Radial hypointensity is seen in the center; B: Axial fat-suppressed T2-weighted MR image shows that the mass is predominantly hyperintense with radial areas of low signal intensity. In addition, intra- and extra-tumoral flow voids can be detected (arrows); C: Sagittal fat-suppressed T2-weighted MR image showing that the rectum is compressed anteriorly by the mass (arrow); D: The mass demonstrated intense heterogeneous enhancement in the arterial phase. The feeding vessels (vascular pedicle) can be demonstrated clearly (arrows); E, F: The mass showed persistent and progressive enhancement in the portal venous (E) and delayed phase (F).

observed in 4 cases and heterogeneous enhancement in 11 cases. In the latter cases, 7 lesions showed necrotic or cystic areas on enhanced CT and/or MR images, and the other 4 lesions demonstrated early non-uniform enhancement with the center showing a radial or fissured region which showed progressive enhancement spreading from the periphery to the center in the portal venous and delayed phases on enhanced MR images (Figures 2D-F, 3C). However, in our case series, there was no statistical difference in the imaging findings between the histologically benign and malignant lesions.

Pathological findings

Of the surgical specimens, 9 tumors were rounded or ovoid, 6 were lobulated, and 10 were encapsulated. The cut surfaces were grayish-white or yellowish-white in color, and fish meat-like in texture. Radial or fissured regions of the abundant fibrotic component were revealed in the center of 4 cases, cystic or necrotic foci in 7 cases, and hemorrhage in one case.

Histological examination demonstrated that the tumors had a haphazard patternless architecture of spindle or ovoid cells with a varying degree of collagenous tis-

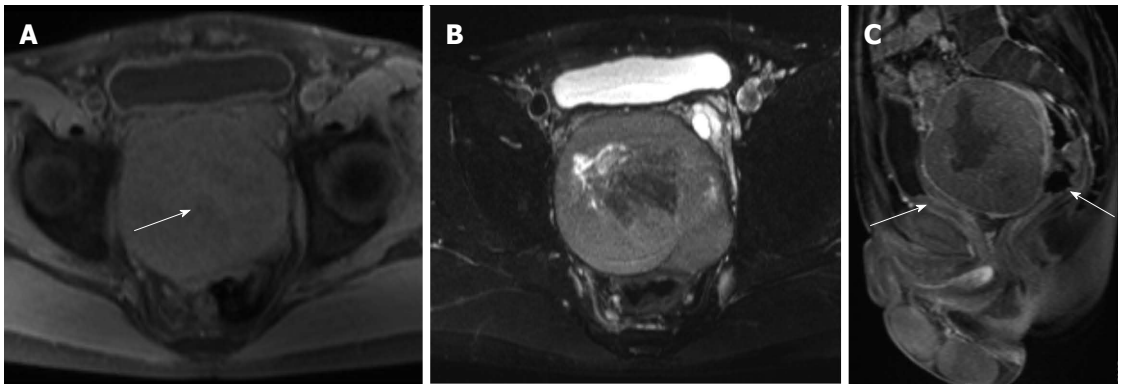

Figure 3 Magnetic resonance images of a solitary fibrous tumor in the rectovesical space. A: T1-weighted Magnetic resonance (MR) image showing an oval isointense mass with patchy mild hyperintensity (arrow). The patchy mild hyperintensity was proven to be a hemorrhage; B: Fat-suppressed T2-weighted MR images reveal a mass with heterogeneous hyperintensity and patchy hypointensity; C: Contrast-enhanced MR images demonstrate moderate heterogeneous enhancement of the mass, which displaces the bladder anteriorly and rectum posteriorly (arrows).

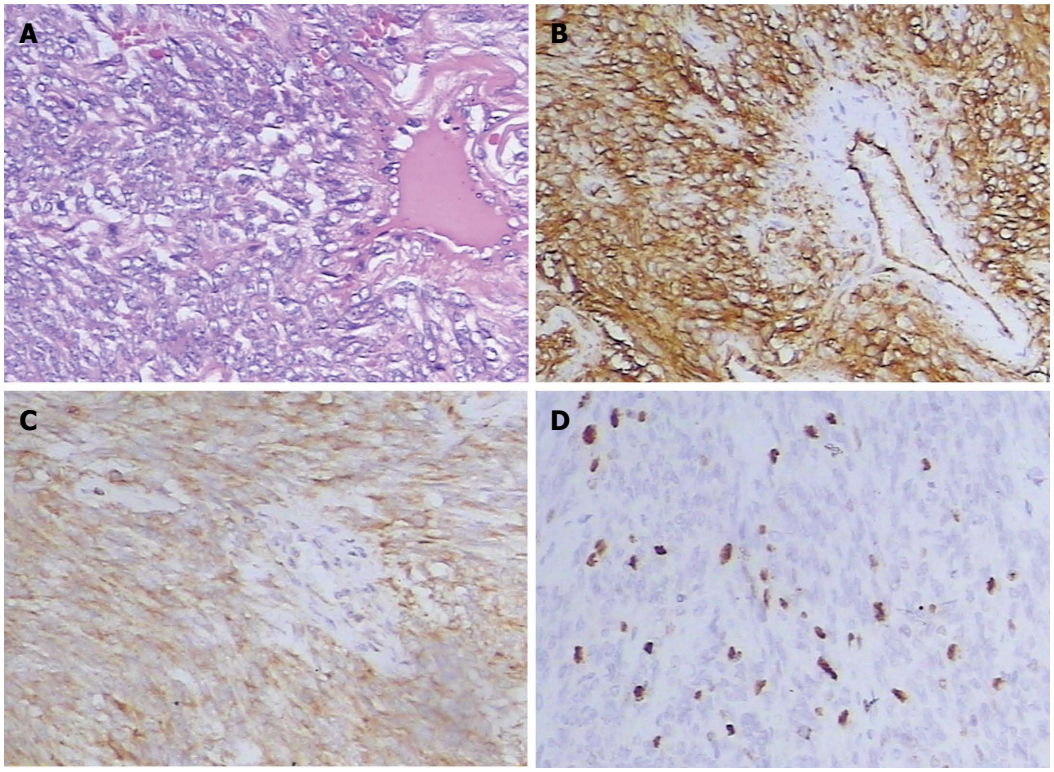

Figure 4 Pathologic features of the solitary fibrous tumor. A: Hematoxylin and eosin staining, × 40, indicates monotonous spindle cell proliferation with a hemangiopericytoma-like vascular growth pattern; B-D: Immunohistochemical staining, x 40, indicates that the tumor is diffusely positive for CD34 (B) and Bcl-2 (C), and the proportion of Ki67 positive cells is 15% (D).

sues and a hemangiopericytoma-like appearance with prominent thin-walled vascular vessels (Figure 4A). The degree of cellularity varied for each tumor and was inversely related to the collagenous tissues. Immunohistochemical staining revealed that CD34 (Figure 4B) was positive in all cases, CD99 in 12 cases, B-cell lymphoma 2 (bcl-2) (Figure 4C) in 14 cases, S-100 in 4 cases, while all lesions were negative for desmin. The proportion of Ki-67 positive cells was greater than 10% in 4 cases (Figure 4D), and less than 5% in the other cases. In total, 8 patients were classified as benign and 7 presented malignant criteria at pathological analysis of the surgical specimens. All 7 malignant tumors were hypercellular lesions, in which 3 each had mild to moderate atypia, and 4 displayed marked atypia.

DISCUSSION

SFT is a rare spindle cell mesenchymal neoplasm with age of onset around 50-60 years, and equal distribution in men and women. Patients in our series ranged from 1 to 76 years, but the incidence was higher in men than in women with a sex ratio of 4:1. To the best of our knowledge, we report the first case of SFT in an infant.

Although SFTs were thought to occur most frequently in the pleura, they may develop virtually anywhere throughout the body, while involvement of the abdomen and pelvis is particularly rare[2]. Despite its characteristic histological and immunohistochemical features, SFTs in the abdomen and pelvis remain a diagnostic challenge to both clinicians and radiologists; it is often poorly recognized and frequently confused with other neoplasms that more commonly occur at this site. Although rare, radiologists and surgeons must be aware of SFTs in the abdomen and pelvis.

Extrapleural SFTs were typically demonstrated as large, slow-growing soft tissue tumors[4]. Symptoms related to the site are frequent in these locations, such as a palpable mass, pain, gross hematuria, bowel obstruction, and urinary retention or obstruction[11,12], as seen in some of our patients. Systemic symptoms such as hypoglycemia (< 5% patients), arthralgia, hypertrophic osteoarthropathy, and clubbing have also been documented in the literature[4,13]; however, they were not present in any of our patients. These symptoms usually resolve upon removal of the tumor.

In the last 20 years, the classification of SFTs and hemangiopericytoma has changed, and most hemangiopericytomas are now thought to be cellular variants of SFTs[2,3]. Overall, SFTs are usually well-demarcated and partially encapsulated in neoplasms[2]. These tumors are highly vascular and have a propensity to undergo hemorrhage, necrosis, and myxoid degeneration. Microscopically, they show a wide range of morphological features, from predominantly fibrous lesions containing alternating fibrous areas and hyalinized thick-walled vessels (fibrous variants) to more cellular and less fibrous neoplasms with a "patternless pattern" (a monotonous appearance) and thin-walled branching vessels (cellular variant)[2,3,14]. Immunohistochemically, both of them variably express CD34, CD99, and bcl-2 antigens; and the fibrous form demonstrates strong reactivity with CD34, whereas the cellular form demonstrates weak reactivity[2].

General histological features that may help to identify a malignant lesion include large size, infiltrative margins, hypercellularity, nuclear atypia, mitotic activity (≥ 4/10 high-power fields), and the presence of necrosis and hemorrhage[2,15,16]. In addition, malignant SFTs tend to lose CD34 immunoreactivity and overexpress Ki-67, P53, and S-100[17]. In our cases, 8 tumors were classified as benign, and 7 as malignant. Although most extrapleural SFTs have been reported to be benign histologically, approximately 10%-15% of SFTs demonstrate malignant behavior in the form of recurrence or metastasis[2,18]. Local recurrences and distant metastases may be expected in malignant SFTs, as seen in three of our patients. Although none were found in our patients, some cases of "histologically benign" SFTs that do recur or metastasize have been reported in the literature[19,20]. The most important risk factor for recurrence is invaded surgical margins. Therefore, complete resection with negative surgical margins is the treatment of choice, and long-term follow-up of all patients is highly recommended, regardless of anatomic location[20,21]. The vascular nature and the presence of large feeding vessels made surgical removal technically difficult and preoperative embolization that can reduce intraoperative hemorrhage may be required[22], as seen in one of our patients.

Radiological information provides useful information, such as detection, characterization, and localization of tumors. In addition, it can depict the local extent, possible invasion into adjacent structures, and locoregional and distant metastases. Importantly, these images provide a road map in the future for the operating surgeons. The most common imaging finding, recently reported in the literature, was a large, well-defined, round, oval, or lobulated hypervascular mass that tended to displace or invade adjacent structures such as the bowel, urinary bladder, seminal vesicle, ureter, and vessels[4,5,12]. The largest mass measured in our cases was 25.1 cm × 15.0 cm. The site of origin of the mass could not be defined on some images because margins blended in with adjacent structures. We inferred that the lobulated shape was due to different growth rates of the tumor. In addition, the difference in the resistance against the growth of the tumor may also be an important factor.

Most of our patients with plain CT scans demonstrated an isodense mass with patchy hypodensity. The attenuation likely depended upon the collagen content, as hyperdense lesions have abundant collagen[6]. Calcification is rare and can be seen in large benign or malignant tumors, but its presence or absence is not necessarily a helpful distinguishing feature[4,6]. On MRI, SFTs were usually isointense or slightly hyperintense on T1WI and heterogeneously hyperintense on T2WI, relative to muscle. Heterogeneous signal intensity was observed in some cases and was likely related to the components of hemorrhage, necrosis, cystic, or myxoid degeneration, and hyalinized stromal content[4,5,7]. However, the presence of low-signal-intensity foci on both T1WI and T2WI were mainly attributed to the components of dense collagen and fibrosis, low cellularity, and associated reduced proton mobility[6]. In addition, lesions with high fibrous content may demonstrate progressive enhancement during the arterial and portal phases that become marked on delayed images[5,8], as seen in some of our patients.

SFTs were highly vascular and vigorously enhancing on both enhanced CT and MR images. These tumors are usually heterogeneous, with hypervascular areas showing early intense enhancement, hypercellular areas showing moderate enhancement, and areas of necrosis or of cystic or myxoid degeneration showing no enhancement[5,23]. In addition, hypercellular areas demonstrated persistent enhancement in the venous and delayed phases. However, there is considerable overlap in the type of enhancement, during which 100% of malignant and 60% of benign SFTs show heterogeneous enhancement[23], as seen in our patients. Enhanced CT and MR images can depict the supplying arteries, and intra- or extra-tumoral flow voids can be readily revealed on unenhanced T2WI.

Wignall *et al*[24] and Garcia-Bennett *et al*[25] thought that the presence of a vascular pedicle, although not specific, is a useful distinguishing feature of SFTs; it was seen in 4 of our patients.

The differential diagnosis for these imaging characteristics includes other hypervascular tumors or tumors with predominant fibrous content, such as leiomyosarcoma, neurogenic tumor, pheochromocytoma, lymphoma, desmoid tumor, malignant fibrous histocytoma, mesothelioma, and fibroma. Using imaging findings alone, differentiating among these is not possible. Therefore, complete excision and histopathologic examination are necessary to establish the diagnosis.

In conclusion, the imaging features of SFTs in the abdomen and pelvis predominantly appeared as well-defined, hypervascular masses with variable degrees of necrosis, cystic change, or hemorrhage. They usually manifested as heterogeneous hyperintensities on T2WI with low signal intensity areas representing flow voids, fibrosis, or collagen. Although we believe that the radiologist may diagnose SFT when a mass presents with the aforementioned imaging features, histopathologic examination remains necessary to confirm the diagnosis.

COMMENTS

Background

Solitary fibrous tumors (SFTs) may occur in any site of the body, but their presence in the abdomen and pelvis is rare. Clinically, they are often misdiagnosed as other hypervascular tumors by radiological and pathologic examination. Few studies to date have investigated the imaging features of SFTs in the abdomen and pelvis.

Research frontiers

The imaging appearance of SFTs on imaging is much less well reported than the histopathologic features. To better characterize the radiological features of this rare disease, the authors present the computed tomography and/or magnetic resonance imaging features of 15 cases of SFTs within the abdomen and pelvis, and correlated them with histopathological results.

Innovations and breakthroughs

This is the largest and most detailed radiologic case series of SFTs in the abdomen and pelvis reported to date.

Applications

This study indicated that the imaging features of SFTs in the abdomen and pelvis predominantly appear as a well-defined, hypervascular mass with a variable degree of necrosis, cystic change, or hemorrhage. They usually manifest as heterogeneous hyperintensity on T2-weighted images with low signal intensity areas representing flow voids, fibrosis, or collagen. The radiologist may suggest the diagnosis of SFTs when a mass with the above imaging features is encountered.

Terminology

SFTs can be benign or malignant and are considered a pathologically diverse, ubiquitous mesenchymal neoplasm of fibroblastic or myofibroblastic origin.

Peer review

This is a retrospective clinical analysis of 15 cases of SFTs in the abdomen and pelvis. SFTs in the abdomen and pelvis are rarely encountered in clinics. Only anecdotal case reports are given in the medical literature. This case series is important and sheds light on these uncommon neoplasms.

REFERENCES

1 **Klemperer P**, Rabin CB. Primary neoplasm of the pleura: a report of five cases. *Arch Pathol* 1931; **11**: 385-412

2 **Gengler C**, Guillou L. Solitary fibrous tumour and haemangiopericytoma: evolution of a concept. *Histopathology* 2006; **48**: 63-74 [PMID: 16359538 DOI: 10.1111/j.1365-2559.2005.02290.x]

3 **Fletcher CD**. The evolving classification of soft tissue tumours: an update based on the new WHO classification. *Histopathology* 2006; **48**: 3-12 [PMID: 16359532 DOI: 10.1111/j.1365-2559.2005.02284.x]

4 **Shanbhogue AK**, Prasad SR, Takahashi N, Vikram R, Zaheer A, Sandrasegaran K. Somatic and visceral solitary fibrous tumors in the abdomen and pelvis: cross-sectional imaging spectrum. *Radiographics* 2011; **31**: 393-408 [PMID: 21415186 DOI: 10.1148/rg.312105080]

5 **Zhang WD**, Chen JY, Cao Y, Liu QY, Luo RG. Computed tomography and magnetic resonance imaging findings of solitary fibrous tumors in the pelvis: correlation with histopathological findings. *Eur J Radiol* 2011; **78**: 65-70 [PMID: 19815359 DOI: 10.1016/j.ejrad.2009.09.001]

6 **Ginat DT**, Bokhari A, Bhatt S, Dogra V. Imaging features of solitary fibrous tumors. *AJR Am J Roentgenol* 2011; **196**: 487-495 [PMID: 21343490 DOI: 10.2214/AJR.10.4948]

7 **Rosenkrantz AB**, Hindman N, Melamed J. Imaging appearance of solitary fibrous tumor of the abdominopelvic cavity. *J Comput Assist Tomogr* 2010; **34**: 201-205 [PMID: 20351504 DOI: 10.1097/RCT.0b013e3181c84154]

8 **Moser T**, Nogueira TS, Neuville A, Riehm S, Averous G, Weber JC, Veillon F. Delayed enhancement pattern in a localized fibrous tumor of the liver. *AJR Am J Roentgenol* 2005; **184**: 1578-1580 [PMID: 15855118 DOI: 10.2214/ajr.184.5.01841578]

9 **Wat SY**, Sur M, Dhamanaskar K. Solitary fibrous tumor (SFT) of the pelvis. *Clin Imaging* 2008; **32**: 152-156 [PMID: 18313582 DOI: 10.1016/j.clinimag.2007.07.003]

10 **Joe BN**, Bolaris M, Horvai A, Yeh BM, Coakley FV, Meng MV. Solitary fibrous tumor of the male pelvis: findings at CT with histopathologic correlation. *Clin Imaging* 2008; **32**: 403-406 [PMID: 18760732 DOI: 10.1016/j.clinimag.2008.02.032]

11 **Gold JS**, Antonescu CR, Hajdu C, Ferrone CR, Hussain M, Lewis JJ, Brennan MF, Coit DG. Clinicopathologic correlates of solitary fibrous tumors. *Cancer* 2002; **94**: 1057-1068 [PMID: 11920476 DOI: 10.1002/cncr.10328]

12 **Yi B**, Bewtra C, Yussef K, Silva E. Giant pelvic solitary fibrous tumor obstructing intestinal and urinary tract: a case report and literature review. *Am Surg* 2007; **73**: 478-480 [PMID: 17521003]

13 **Fridlington J**, Weaver J, Kelly B, Kelly E. Secondary hypertrophic osteoarthropathy associated with solitary fibrous tumor of the lung. *J Am Acad Dermatol* 2007; **57**: S106-S110 [PMID: 17938018 DOI: 10.1016/j.jaad.2006.10.045]

14 **Ide F**, Obara K, Mishima K, Saito I, Kusama K. Ultrastructural spectrum of solitary fibrous tumor: a unique perivascular tumor with alternative lines of differentiation. *Virchows Arch* 2005; **446**: 646-652 [PMID: 15909170 DOI: 10.1007/s00428-005-1261-z]

15 **England DM**, Hochholzer L, McCarthy MJ. Localized benign and malignant fibrous tumors of the pleura. A clinicopathologic review of 223 cases. *Am J Surg Pathol* 1989; **13**: 640-658 [PMID: 2665534 DOI: 10.1097/00000478-198908000-00003]

16 **Vallat-Decouvelaere AV**, Dry SM, Fletcher CD. Atypical and malignant solitary fibrous tumors in extrathoracic locations: evidence of their comparability to intra-thoracic tumors. *Am J Surg Pathol* 1998; **22**: 1501-1511 [PMID: 9850176 DOI: 10.1097/00000478-199812000-00007]

17 **Yokoi T**, Tsuzuki T, Yatabe Y, Suzuki M, Kurumaya H, Koshikawa T, Kuhara H, Kuroda M, Nakamura N, Nakatani Y, Kakudo K. Solitary fibrous tumour: significance of p53 and CD34 immunoreactivity in its malignant transformation. *Histopathology* 1998; **32**: 423-432 [PMID: 9639117 DOI: 10.1046/j.1365-2559.1998.00412.x]

18 **Daigeler A**, Lehnhardt M, Langer S, Steinstraesser L, Steinau HU, Mentzel T, Kuhnen C. Clinicopathological findings in a case series of extrathoracic solitary fibrous tumors of

soft tissues. *BMC Surg* 2006; **6**: 10 [PMID: 16824225 DOI: 10.1186/1471-2482-6-10]
19 **Hasegawa T**, Matsuno Y, Shimoda T, Hasegawa F, Sano T, Hirohashi S. Extrathoracic solitary fibrous tumors: their histological variability and potentially aggressive behavior. *Hum Pathol* 1999; **30**: 1464-1473 [PMID: 10667425 DOI: 10.1016/S0046-8177(99)90169-7]
20 **Cranshaw IM**, Gikas PD, Fisher C, Thway K, Thomas JM, Hayes AJ. Clinical outcomes of extra-thoracic solitary fibrous tumours. *Eur J Surg Oncol* 2009; **35**: 994-998 [PMID: 19345055 DOI: 10.1016/j.ejso.2009.02.015]
21 **Park MS**, Araujo DM. New insights into the hemangiopericytoma/solitary fibrous tumor spectrum of tumors. *Curr Opin Oncol* 2009; **21**: 327-331 [PMID: 19444101 DOI: 10.1097/CCO.0b013e32832c9532]
22 **Zerón-Medina J**, Rodríguez-Covarrubias F, García-Mora A, Guerrero-Hernandez M, Chablé-Montero F, Albores-Saavedra J, Medina-Franco H. Solitary fibrous tumor of the pelvis treated with preoperative embolization and pelvic exenteration. *Am Surg* 2011; **77**: 112-113 [PMID: 21396319]
23 **Rosado-de-Christenson ML**, Abbott GF, McAdams HP, Franks TJ, Galvin JR. From the archives of the AFIP: Localized fibrous tumor of the pleura. *Radiographics* 2003; **23**: 759-783 [PMID: 12740474 DOI: 10.1148/rg.233025165]
24 **Wignall OJ**, Moskovic EC, Thway K, Thomas JM. Solitary fibrous tumors of the soft tissues: review of the imaging and clinical features with histopathologic correlation. *AJR Am J Roentgenol* 2010; **195**: W55-W62 [PMID: 20566782 DOI: 10.2214/AJR.09.3379]
25 **Garcia-Bennett J**, Olivé CS, Rivas A, Domínguez-Oronoz R, Huguet P. Soft tissue solitary fibrous tumor. Imaging findings in a series of nine cases. *Skeletal Radiol* 2012; **41**: 1427-1433 [PMID: 22349595 DOI: 10.1007/s00256-012-1364-y]

P- Reviewers: Beltran MA, Youn HS **S- Editor**: Ma YJ
L- Editor: Cant MR **E- Editor**: Ma S

百世登
Baishideng®

Published by **Baishideng Publishing Group Co., Limited**
Flat C, 23/F., Lucky Plaza,
315-321 Lockhart Road, Wan Chai, Hong Kong, China
Fax: +852-65557188
Telephone: +852-31779906
E-mail: bpgoffice@wjgnet.com
http://www.wjgnet.com

ISSN 1007-9327
17>